IEEE Photonics Journal
An IEEE Photonics Society Publication

Open Access

Widely Tunable Single-Passband Microwave Photonic Filter Based on DFB-SOA-Assisted Optical Carrier Recovery

Volume 7, Number 5, October 2015

Ye Deng
Ming Li
Jian Tang
Shuqian Sun
Ningbo Huang
Ninghua Zhu

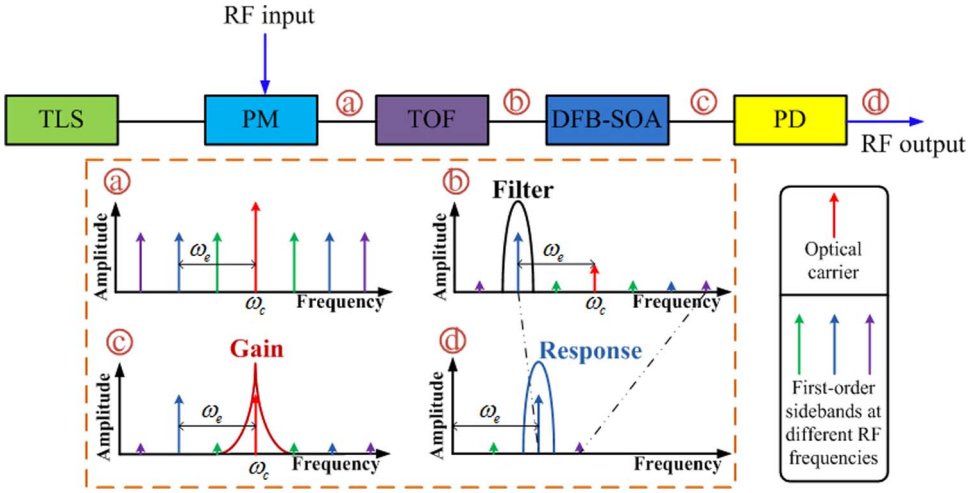

DOI: 10.1109/JPHOT.2015.2475612
1943-0655

IEEE photonics SOCIETY

IEEE

Widely Tunable Single-Passband Microwave Photonic Filter Based on DFB-SOA-Assisted Optical Carrier Recovery

Ye Deng, Ming Li, Jian Tang, Shuqian Sun, Ningbo Huang, and Ninghua Zhu

Institute of Semiconductors, Chinese Academy of Sciences, Beijing 100083, China

DOI: 10.1109/JPHOT.2015.2475612

Manuscript received August 5, 2015; revised August 28, 2015; accepted August 28, 2015. Date of publication September 1, 2015; date of current version September 16, 2015. This work was supported in part by the National Natural Science Foundation of China under Grant 61377002, Grant 61321063, and Grant 61090391 and in part by Beijing Natural Science Foundation under Grant 4152052. The work of M. Li was supported in part by the "Thousand Young Talent" program. Corresponding author: M. Li (e-mail: ml@semi.ac.cn).

Abstract: A widely tunable single-passband microwave photonic filter (MPF) based on a distributed-feedback semiconductor optical amplifier (DFB-SOA) is proposed and experimentally demonstrated in this paper. The fundamental principle is to recover the suppressed optical carrier from a passband optical filter by the wavelength-selective amplification via a DFB-SOA. A microwave signal is then generated by beating the recovered optical carrier with the phase-modulated lower sideband, and thus, an MPF is achieved with the shape of the passband optical filter that is mapped from the optical domain to the electrical domain. By tuning the central wavelength of the passband optical filter, a single-passband MPF with a frequency tuning range from 5 to 35 GHz is obtained. The 3-dB bandwidth and the out-of-band suppression ratio are measured to be 4 GHz and 20 dB, respectively. In addition, the tunability of the MPF that is dependent on the driven current of the DFB-SOA is also experimentally investigated.

Index Terms: Radio frequency photonics, laser amplifiers, frequency filtering.

1. Introduction

Microwave photonic filters (MPFs) have attracted considerable interest over the past few years thanks to the advantageous features such as large frequency coverage, flexible tunability, light weight, and immunity to electromagnetic interference [1]–[5]. Therefore, for many applications in wireless communication, modern radar, and electronic warfare systems, MPFs are highly desired for processing broadband and high-frequency microwave signals and are comparable to conventional electrical filters [6]. Typical techniques for realizing MPFs are based on optical delay line structures [7]–[9]. However, due to the nature of the discrete time signal processing, multiple harmonic passbands are achieved with poor tunability. In the past years, the realization of a single passband MPF with wideband tunability is of great interest for its important use in microwave signal processing application. Many approaches have been reported to achieve a single passband MPF by using a broad optical source combing with a spectrum slicer such as a Mach–Zehnder

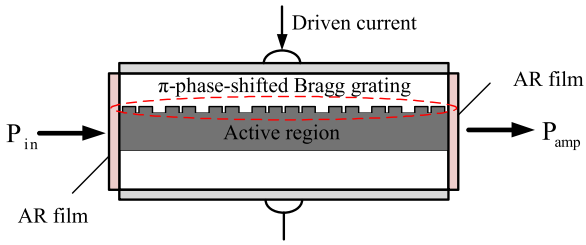

Fig. 1. Schematic diagram of the DFB-SOA.

interferometer (MZI) or a Waveshaper [10]–[12]. However, the MZI without well-designed packaging is sensitive to the ambient changes and the Waveshaper is costly and bulky. A single bandpass MPF can also be realized based on phase modulation to intensity modulation (PM–IM) conversion, using a Fabry–Pérot laser diode [13], a ring resonator [14], [15], fiber Bragg gratings (FBGs) [16]–[19], or stimulated Brillouin scattering (SBS) in a nonlinear fiber [20]–[23]. By filtering or amplifying one of the modulated sidebands, the phase modulated signals can be transferred to the intensity modulated signals and thus the shape of the optical filter or amplifier can be mapped to the amplitude response of the MPF. In [17], a tunable single passband MPF using a phase-shifted FBG was obtained. However, the frequency tuning range is restricted by the bandwidth of the phase-shifted FBG. Furthermore, since this scheme must filter the remaining sideband while keeping a strong optical carrier and, thus, results in a challenge of freedom in passband shape design, tuning range, and device complexity. To overcome the limitation, a tunable single passband MPF based on Brillouin-assisted optical carrier recovery in a high nonlinear fiber was proposed [22]. The central frequency of the MPF can be tuned over a wide range from 9.5 to 32.5 GHz by simply adjusting the wavelength of the optical carrier. However, due to the use of the frequency shifter for the optical carrier recovering based on SBS amplification, the system is costly and complex.

In this paper, we propose a novel approach to implementing a widely tunable single passband MPF based on a distributed-feedback semiconductor optical amplifier (DFB-SOA). A DFB-SOA is related to a DFB laser biased below lasing threshold that combines the functions of optical spectrum selectivity and optical power amplification [24]. The proposed MPF is realized by mapping the shape of a tunable optical passband filter from the optical domain to the electrical domain. When the phase modulated signal is sent into the optical filter, the lower sideband will pass through it while the optical carrier and the upper sideband are significantly suppressed. After that, the optical carrier is then recovered owe to the wavelength-selective amplification of the DFB-SOA. Through PM–IM conversion, a microwave signal is generated at the photodetector. The proposed MPF is theoretically analyzed and experimentally demonstrated. By tuning the central wavelength of the tunable optical passband filter, a frequency tuning range from 5 to 35 GHz is achieved. The 3-dB bandwidth and the out-of-band suppression ratio are 4 GHz and 20 dB, respectively. Additionally, the tunability of the MPF dependent on the driven current of the DFB-SOA is also experimentally investigated. It worth noting that the 3-dB bandwidth can be largely reduced by using an optical filter with narrow bandwidth, such as a π-phase-shifted FBG or a high-Q micro-ring resonator. Furthermore, our proposed MPF also shows a potential application as an optical vector network analyzer (OVNA).

2. Principle

The key device of our proposed MPF is DFB-SOA. The schematic diagram of the DFB-SOA is shown in Fig. 1. As can be seen, two concatenated identical uniform fiber Bragg gratings (FBGs) with a central π-phase-shift between them are built outside the active layer of the DFB-SOA. Both the front and rear facets of the phase-shifted DFB-SOA are coated with antireflection (AR) films and thus the input optical signal can pass through the device. An external current is injected into the phase-shifted DFB-SOA to adjust the gain of the active layer.

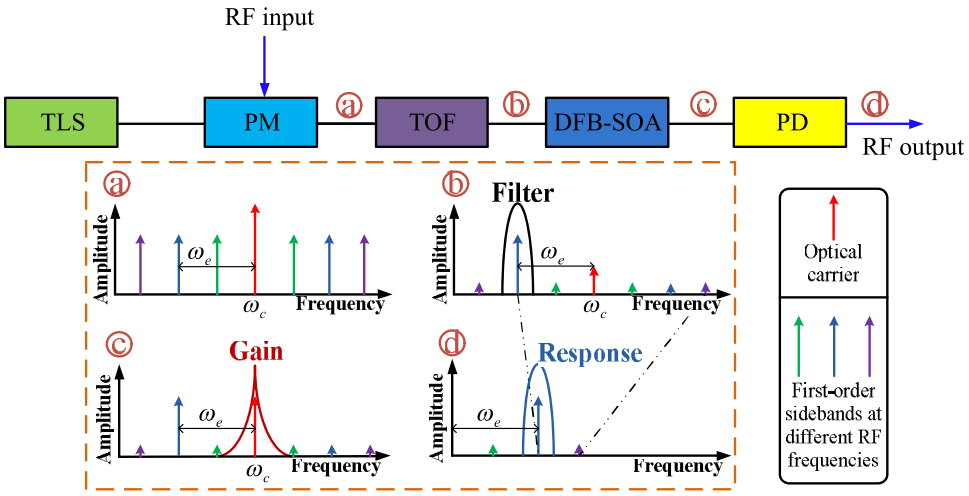

Fig. 2. Schematic diagram of the proposed MPF based on a DFB-SOA.

According to the coupled-mode equations and transfer-matrix method, the gain spectrum of the DFB-SOA can be obtained as [25]

$$G(\omega) = \frac{1}{\left\{ j\frac{k^2}{\gamma^2}\sinh^2(\gamma l) - j\left[\cosh(\gamma l) - j\frac{\sigma}{\gamma}\sinh(\gamma l)\right]^2 \right\}} \tag{1}$$

where $j = \sqrt{-1}$, and ω represents the optical angular frequency. k is the coupling coefficient, l is the length of the FBG, and $\gamma = \sqrt{k^2 - \sigma^2}$. σ denotes the complex detuning, which is defined by

$$\sigma = n_{\text{eff}}\frac{\omega}{c} - \frac{\pi}{\Lambda} - \frac{g}{2}\alpha - j\frac{g - \alpha_{\text{int}}}{2} \tag{2}$$

where n_{eff} is the effective mode refractive index, c is the velocity of light in vacuum, Λ is the grating period, and α is linewidth enhancement factor of active layer. $g = \Gamma a N_0(I/I_0 - 1)$ is the power gain coefficient in unsaturated condition. Γ is the confinement factor, a is the differential gain, N_0 is the carrier density at transmission, I_0 is the current required to reach transparency, and α_{int} is the internal loss coefficient. Therefore, it can be seen from (1) and (2) that the gain spectrum of the DFB-SOA is dependent on the injected current. By simply controlling the injected current, the resonant wavelength can be shifted and power gain can be changed.

The schematic diagram of the proposed tunable single passband MPF is shown in Fig. 2, consisting of a tunable laser source (TLS), a phase modulator (PM), a tunable optical filter (TOF), a DFB-SOA and a photodetector (PD). In the proposed MPF, a continuous wave (CW) lightwave from the TLS is sent to the PM to be phase modulated by a microwave signal. The phase modulated signal is then directed to the TOF which has a bandpass response with a central frequency deviated from the optical carrier. Within the TOF, the lower sideband which is located in the passband passes while the optical carrier and the upper sideband which are located in the stopband are deeply suppressed. The optical carrier-suppressed single-sideband signal is then launched into the DFB-SOA. When the suppressed optical carrier falls in the range of the gain spectrum of the DFB-SOA, it will be recovered as the result of the wavelength-selective amplification of the DFB-SOA. Through PM–IM conversion, a microwave signal will be generated at the PD by beating the recovered optical carrier and the lower sideband. In our scheme, the magnitude of the generated microwave signal varies with the magnitude of the lower sideband corresponding to the transmission response of the TOF, and thus the MPF can be achieved with the shape of the passband of the TOF which is mapped from the optical domain to the electrical domain. The central frequency of our proposed MPF is dependent on the frequency

spacing between the optical carrier and the central wavelength of the TOF. By changing the central wavelength of the TOF or adjusting the optical carrier and the gain spectrum of the DFB-SOA simultaneously, the central frequency of the single passband of the MPF could be tuned. The bandwidth of the MPF is determined by that of the TOF.

Mathematically, the optical field at the PM under small-signal modulation is described as [26]

$$\begin{aligned} E_{\mathrm{PM}}(t) &= A\exp[j\omega_c t + j\beta\cos(\omega_e t)] \\ &\approx AJ_0(\beta)\exp(j\omega_c t) + AJ_1(\beta)\exp[j(\omega_c t + \omega_e t)] + AJ_{-1}(\beta)\exp[j(\omega_c t - \omega_e t)] \end{aligned} \tag{3}$$

where A is the amplitude of the optical carrier from the TLS. ω_c and ω_e denote the angular frequency of the optical carrier and the microwave signal, respectively. $J_n(\cdot)$ is the nth order of the first kind Bessel functions and β is the phase modulation index of the PM.

By applying the Fourier transform to (3), the output optical signal from phase modulator in frequency domain can be written as

$$E_{\mathrm{PM}}(\omega) = 2\pi AJ_0(\beta)\delta(\omega - \omega_c) + 2\pi AJ_1(\beta)\delta[\omega - (\omega_c + \omega_e)] + 2\pi AJ_{-1}(\beta)\delta[\omega - (\omega_c - \omega_e)]. \tag{4}$$

Assuming the magnitude response of the TOF is $H(\omega)$, which is centered at $\omega_c - \omega_e$ with a single-passband shape, the optical carrier-suppressed single-sideband signal output from the TOF can be expressed as

$$E_{\mathrm{TOF}}(\omega) = 2\pi AJ_0(\beta)H(\omega_c)\delta(\omega - \omega_c) + 2\pi AJ_{-1}(\beta)H(\omega_c - \omega_e)\delta[\omega - (\omega_c - \omega_e)]. \tag{5}$$

The optical carrier-suppressed single-sideband signal is then launched into the DFB-SOA. When the residual optical carrier is located in the range of the gain spectrum, it will be amplified by the DFB-SOA. The optical carrier recovered signal output from the DFB-SOA can be expressed as

$$E_{\mathrm{DFB}}(\omega) = 2\pi AJ_0(\beta)G(\omega_c)H(\omega_c)\delta(\omega - \omega_c) + 2\pi AJ_{-1}(\beta)H(\omega_c - \omega_e)\delta[\omega - (\omega_c - \omega_e)]. \tag{6}$$

When $G(\omega_c)H(\omega_c) > 1$, the suppressed optical carrier could be effectively recovered by the DFB-SOA. After square-law detection in the PD, the output microwave photocurrent for ω_e component can be obtained as

$$i(\omega_e) = C \cdot H(\omega_c - \omega_e) \tag{7}$$

where $C = 4\pi^2 A^2 J_0(\beta)J_{-1}(\beta)G(\omega_c)H(\omega_c)$ is a constant since it is the product of the magnitude response of the optical filter and the DFB-SOA at the fixed frequency. The gain coefficient G could be increased by tuning the injected current of the DFB-SOA. It can be clearly seen from (7) that the phase modulated optical signal is converted to a microwave signal through PM–IM conversion and thus the shape of the passband of the TOF is mapped from optical domain to electrical domain. The central frequency of the proposed MPF is dependent on the frequency space between the optical carrier and the central wavelength of the TOF. The tunable frequency coverage is limited by the bandwidth of the PM and the PD.

3. Experiment

The experimental setup for measuring the transmission response of the proposed tunable single passband MPF is shown in Fig. 3. The lasing threshold of the DFB-SOA is measured to be 23.1 mA. The gain spectrum of the DFB-SOA with an injection current of 23 mA is shown in Fig. 4. It can be seen that the gain peak is located at 1546.39 nm. A CW lightwave from a TLS (Agilent 8164B) with optical power of 14 dBm is sent to a PM via a polarization controller (PC). The central wavelength of the lightwave is tuned to match the gain peak of the DFB-SOA. The polarization state of the lightwave is adjusted by the PC to minimize the polarization-dependent loss. The PM with a bandwidth of 40 GHz and a half-wave voltage of 6 V is driven by a sinusoidal microwave signal from a vector network analyzer (VNA Agilent 8722ET) with a fixed power of -5 dBm. At the output of the PM, the phase modulated signal is launched into a TOF (Yenista

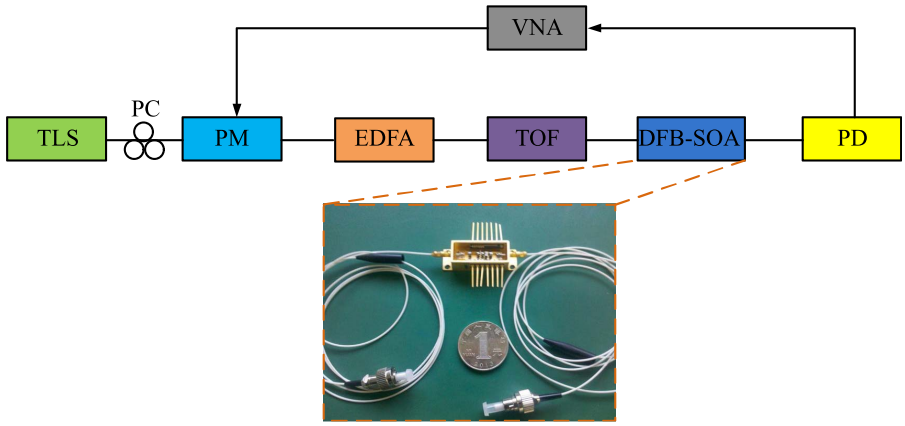

Fig. 3. Experiment setup for measuring the transmission response of the proposed MPF.

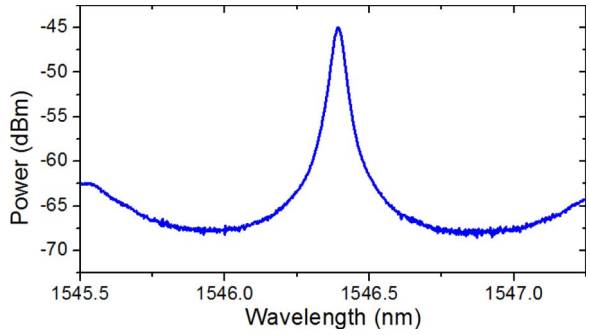

Fig. 4. Measured gain spectrum of the DFB-SOA with driven current of 23 mA.

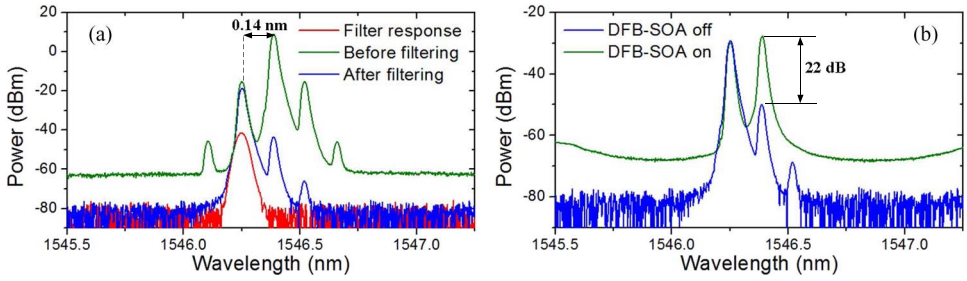

Fig. 5. Measured optical spectrum of the optical signal. (a) Before and after the TOF. (b) With and without the wavelength-selective amplification of the DFB-SOA.

XTA-50) with a 3-dB bandwidth of 32 pm (i.e., 4 GHz) via an erbium-doped optical fiber amplifier (EDFA). The EDFA amplifies the phase modulated signal to 22 dBm to compensate the insertion loss of the TOF. The central wavelength of the TOF is firstly set to be 1546.25 nm. When the microwave frequency output from the VNA is equal to the frequency spacing between the optical carrier and the central wavelength of the TOF (i.e., 17.5 GHz), the lower sideband will pass directly while the optical carrier and the upper sideband will be significant suppressed. Fig. 5(a) shows the output optical spectrum from the TOF when a CW electrical signal with fixed frequency of 17.5 GHz is applied to the PM. It can be obviously seen that the lower sideband remain unchanged while the optical carrier is deeply suppressed more than 50 dB. The filtered optical signal is then directed to the DFB-SOA for wavelength-selective amplification. The insertion loss of the DFB-SOA is about 10 dB. The output optical spectrum from the DFB-SOA is shown

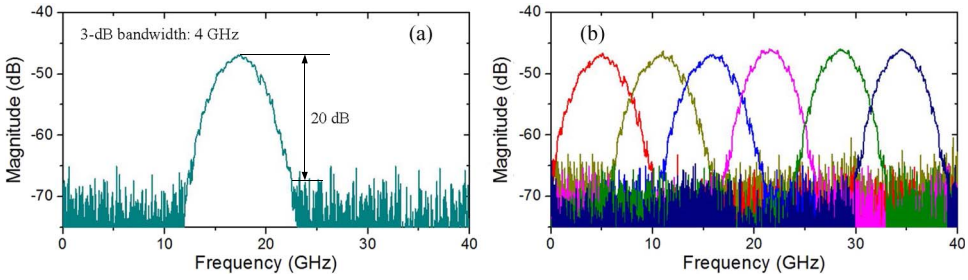

Fig. 6. Measured magnitude response of the MPF (a) with the central frequency of 17.5 GHz and (b) with frequency tuning range from 5 to 35 GHz.

in Fig. 5(b), corresponding to the case that the DFB-SOA is on (green) and off (blue). It can be clearly observed that the suppressed optical carrier is effectively recovered about 22 dB. The output optical signal from the DFB-SOA is then injected to a PD with a bandwidth of 40 GHz. Through PM–IM conversion, a microwave signal at the output of the PD is generated, and it is then sent back to the VNA for frequency response measurement.

Fig. 6(a) shows the measured magnitude response of the proposed MPF by sweeping the frequency of the modulation signal from 50 MHz to 40 GHz. The central frequency of the passband is 17.5 GHz, which shows a good agreement with the frequency spacing between the optical carrier and the central wavelength of the TOF. Moreover, the 3-dB bandwidth of the passband of the MPF is equal to the one of the TOF indicates that the shape of the TOF is directly mapped from the optical domain to the electrical domain. Additionally, the out-of-band suppression ratio of the MPF is measured to be around 20 dB, which is high enough in most applications. It is worth noting that the ripples in the passband may be resulted from the phase fluctuation induced by the spontaneous emission of the DFB-SOA. The out-of-band suppression is mainly determined by the amplification characteristics of the DFB-SOA. The tunability of the central frequency of the MPF is achieved by tuning the central wavelength of the TOF. As can be seen from Fig. 6(b), the tunable center frequency of the passband covers a range from 5 to 35 GHz. It is noted that the tunable frequency coverage here is greatly limited by the bandwidth of the PM and the PD. Thus, the tunable frequency coverage can be further extended by employing a PM and a PD with a wider bandwidth. The total insertion loss of the MPF is about 45 dB. The large insertion loss is mainly caused by the large loss of the TOF and the low optical-electrical conversion efficiency of the PD. By using a high-power handing PD, the insertion loss can be greatly reduced. Besides, the 3-dB bandwidth of the passband is largely dependent on the one of the TOF. If a narrow bandpass optical filter such as a π-phase-shifted FBG or a high-Q micro-ring resonator is employed, the bandwidth of the passband of our proposed MPF could be as narrow as hundreds of MHz. Considering the wavelength shift under optical injection of the DFB-SOA [27], the central wavelength of the TLS should be tuned correspondingly to match the gain peak to make the gain maximum. Furthermore, the proposed tunable single passband MPF can also be regarded as a high-resolution OVNA [28], [29], which offers major advantage of characterizing the transmission response of the optical component with bandpass response.

As far as is known, the gain spectrum of the DFB-SOA will shift when the driven current is changed [30]. Therefore, the tunability of our proposed single passband MPF can also be achieved by tuning the driven current and adjusting the central wavelength of the optical carrier to match the gain peak simultaneously. In order to verify the idea, another experiment based on the same configuration is carried out and investigated. Fig. 7(a) shows the measured gain spectrum of the DFB-SOA biased at different current. It can be observed that, when the driven current is closer to the lasing threshold of the DFB-SOA, the peak gain becomes larger and the passband becomes narrower. Besides, as can be seen, the gain peak shifts from 1546.49 to 1546.39 nm corresponding to the driven current tuned from 20 to 23 mA. The gain peak shifts toward the shorter wavelength side with the increasing driven current due to the refractive index change in active region from carrier injection. The corresponding magnitude response of the

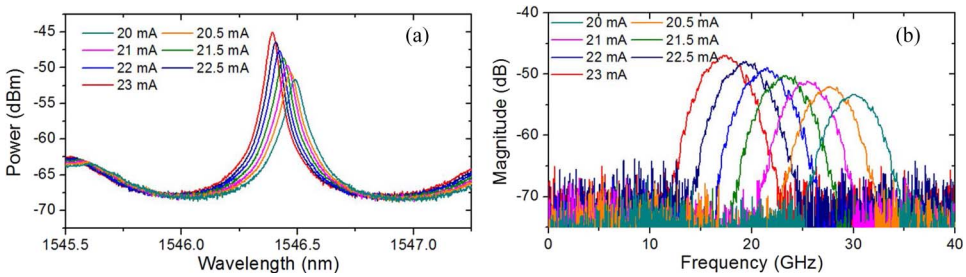

Fig. 7. (a) Measured gain spectrum of the DFB-SOA and (b) the corresponding magnitude response of the MPF under different driven current.

proposed MPF is shown in Fig. 7(b). As can be seen, a single passband with a tunable range from 17.5 to 30 GHz is obtained. The central frequency of the passband is determined by the frequency space between the gain peak and the central wavelength of the TOF which is fixed to be 1546.25 nm. In addition, the out-of-band suppression ratio of the MPF is deteriorated with the decrease of the driven current of the DFB-SOA. This is resulted from the reduced magnitude of the optical carrier due to the decrease of the gain peak. If a SOA is employed before the PD to adjust the power of the optical signal, the out-of-band suppression ratio of the MPF under different driven current could be consistent. Furthermore, if the EDFA and the TOF used in our experiment are replaced by SOA and waveguide filter respectively, our proposed system can be implemented on a single chip using InP/InGaAsP platform [31], [32]. Therefore, our proposed tunable single passband MPF may provide a simple and effective solution for microwave filtering applications.

4. Conclusion

We have proposed a novel approach to implementing a widely tunable single passband MPF based on a DFB-SOA in this paper. The proposed MPF is realized by utilizing the wavelength-selective amplification of the DFB-SOA and mapping the passband of a TOF from the optical domain to the electrical domain. The TOF is used to pass the lower sideband of the phase modulated signal and suppress the optical carrier. The suppressed optical carrier is then effectively recovered by the DFB-SOA and beats with the lower sideband to generate a microwave signal. Through PM–IM conversion, a single passband MPF is obtained with the shape of the TOF. The bandwidth, tunability, insertion loss, and out-of-band suppression ratio of the proposed MPF were investigated in the experiment. By tuning the central wavelength of the TOF, a single passband MPF with frequency tuning range from 5 to 35 GHz was achieved. The 3-dB bandwidth and the out-of-band suppression ratio were measured to be 4 GHz and 20 dB, respectively. The tunable frequency coverage can be further extended by increasing the bandwidth of the PM and the PD. Furthermore, the 3-dB bandwidth can be largely reduced by using an optical passband filter with narrow bandwidth. In addition, the tunability of the MPF dependent on the driven current of the DFB-SOA was also experimentally demonstrated. By tuning the driven current of the DFB-SOA and adjusting the central wavelength of the optical carrier simultaneously, a frequency tuning range from 17.5 to 30 GHz was obtained. Finally, our proposed MPF also shows the potential for integration, which may provide a simple and effective solution for microwave filtering applications.

References

[1] J. Capmany and D. Novak, "Microwave photonics combines two worlds," *Nat. Photon.*, vol. 1, pp. 319–330, 2007.
[2] J. Yao, "Microwave photonics," *J. Lightw. Technol.*, vol. 27, no. 3, pp. 314–335, Feb. 2009.
[3] A. J. Seeds, "Microwave photonics," *IEEE Trans. Microw. Theory Tech.*, vol. 50, no. 3, pp. 877–887, Mar. 2002.
[4] M. Li, J. Azaña, N. Zhu, and J. Yao, "Recent progresses on optical arbitrary waveform generation," *Frontiers Optoelectron.*, vol. 7, no. 3, pp. 359–375, 2014.

[5] H. Jiang *et al.*, "Photonic generation of microwave signals with tunabilities," *Chin. Sci. Bull.*, vol. 59, no. 22, pp. 2672–2683, 2014.
[6] J. Marti and A. Griol, "Harmonic suppressed microstrip multistage coupled ring bandpass filters," *Electron. Lett.*, vol. 34, no. 22, pp. 2140–2142, Oct. 1998.
[7] R. A. Minasian, "Photonic signal processing of microwave signals," *IEEE Trans. Microw. Theory Tech.*, vol. 54, no. 2, pp. 832–846, Feb. 2006.
[8] X. Zou, W. Li, W. Pan, L. Yan, and J. Yao, "Photonic-assisted microwave channelizer with improved channel characteristics based on spectrum-controlled stimulated Brillouin scattering," *IEEE Trans. Microw. Theory Tech.*, vol. 61, no. 9, pp. 3470–3478, Sep. 2013.
[9] J. Leng, W. Zhang, and J. A. R. Williams, "Optimization of superstructured fiber Bragg gratings for microwave photonic filters response," *IEEE Photon. Technol. Lett.*, vol. 16, no. 7, pp. 1736–1738, Jul. 2004.
[10] J. Mora *et al.*, "Photonic microwave tunable single-bandpass filter based on a Mach–Zehnder interferometer," *J. Lightw. Technol.*, vol. 24, no. 7, pp. 2500–2509, Jul. 2006.
[11] M. Li, W. Li, and J. P. Yao, "A tunable optoelectronic oscillator based on a high-Q spectrum-sliced photonic microwave transversal filter," *IEEE Photon. Technol. Lett.*, vol. 24, no. 14, pp. 1251–1253, Jul. 2012.
[12] H. Wang *et al.*, "Widely tunable single-bandpass microwave photonic filter based on polarization processing of a nonsliced broadband optical source," *Opt. Lett.*, vol. 38, no. 22, pp. 4857–4860, Nov. 2013.
[13] Y. Yu *et al.*, "Single passband microwave photonic filter with continuous wideband tunability based on electro-optic phase modulator and Fabry–Pérot semiconductor optical amplifier," *J. Lightw. Technol.*, vol. 29, no. 23, pp. 3542–3550, Dec. 2011.
[14] J. Palací, G. E. Villanueva, J. V. Galán, J. Martí, and B. Vidal, "Single bandpass photonic microwave filter based on a notch ring resonator," *IEEE Photon. Technol. Lett.*, vol. 22, no. 17, pp. 1276–1278, Sep. 2010.
[15] G. D. Kim and S. S. Lee, "Photonic microwave channel selective filter incorporating a thermooptic switch based on tunable ring resonators," *IEEE Photon. Technol. Lett.*, vol. 19, no. 13, pp. 1008–1010, Jul. 2007.
[16] X. Yi and R. A. Minasian, "Microwave photonic filter with single bandpass response," *Electron. Lett.*, vol. 45, no. 7, pp. 362–363, Mar. 2009.
[17] W. Li, M. Li, and J. Yao, "A narrow-passband and frequency-tunable microwave photonic filter based on phase-modulation to intensity-modulation conversion using a phase-shifted fiber Bragg grating," *IEEE Trans. Microw. Theory Tech.*, vol. 60, no. 5, pp. 1287–1296, May 2012.
[18] Y. Deng, M. Li, N. Huang, and N. Zhu, "Ka-band tunable flat-top microwave photonic filter using a multiphase-shifted fiber Bragg grating," *IEEE Photon. J.*, vol. 6, no. 4, pp. 1–8, Aug. 2014.
[19] T. Chen, X. Yi, L. Li, and R. A. Minasian, "Single passband microwave photonic filter with wideband tunability and adjustable bandwidth," *Opt. Lett.*, vol. 37, no. 22, pp. 4699–4701, 2012.
[20] W. Zhang and R. A. Minasian, "Widely tunable single-passband microwave photonic filter based on stimulated Brillouin scattering," *IEEE Photon. Technol. Lett.*, vol. 23, no. 23, pp. 1775–1777, Dec. 2011.
[21] R. Tao, X. Feng, Y. Cao, Z. Li, and B. Guan, "Widely tunable single bandpass microwave photonic filter based on phase modulation and stimulated Brillouin scattering," *IEEE Photon. Technol. Lett.*, vol. 24, no. 13, pp. 1097–1099, Jul. 2012.
[22] W. Wang *et al.*, "Widely tunable single bandpass microwave photonic filter based on Brillouin-assisted optical carrier recovery," *Opt. Exp.*, vol. 22, no. 24, pp. 29 304–29 313, 2014.
[23] Y. Xiao *et al.*, "An ultrawide tunable range single passband microwave photonic filter based on stimulated Brillouin scattering," *Opt. Exp.*, vol. 21, no. 3, pp. 2718–2726, 2013.
[24] Z. Wang, T. Durhuus, B. Mikkelsen, and K. E. Stubkjaer, "Distributed feedback laser amplifiers combining the functions of amplifiers and channel filters," *Appl. Phys. Lett.*, vol. 64, pp. 2065–2067, 1994.
[25] X. Jia, X. Ji, C. Xu, Z. Wang, and W. Zhang, "Analysis of all-optical temporal integrator employing phased-shifted DFB-SOA," *Opt. Exp.*, vol. 22, no. 23, pp. 28 530–28 536, Nov. 2014.
[26] G. Qi, J. Yao, J. Seregelyi, C. Bélisle, and S. Paquet, "Optical generation and distribution of continuously tunable millimeter-wave signals using an optical phase modulator," *J. Lightw. Technol.*, vol. 23, no. 9, pp. 2687–2695, Sep. 2005.
[27] K. Magari, H. Kawaguchi, K. Oe, and M. Fukuda, "Optical narrow-band filters using optical amplification with distributed feedback," *IEEE J. Quantum Electron.*, vol. 24, no. 11, pp. 2178–2190, Nov. 1988.
[28] T. Qing, M. Xue, M. Huang, and S. Pan, "Measurement of optical magnitude response based on double-sideband modulation," *Opt. Lett.*, vol. 39, no. 21, pp. 6174–6176, 2014.
[29] W. Wang *et al.*, "Optical vector network analyzer with improved accuracy based on Brillouin-assisted optical carrier processing," *IEEE Photon. J.*, vol. 6, no. 6, pp. 1–10, Dec. 2014.
[30] Z. Wu, G. Xia, and X. Jia, "Nonuniform DFB-SOAs: Dynamic characteristics of bistability and a novel configuration based on linearly variable current injection," *IEEE J. Quantum Electron.*, vol. 41, no. 3, pp. 384–389, Mar. 2005.
[31] D. Marpaung *et al.*, "Integrated microwave photonics," *Laser Photon. Rev.*, vol. 7, no. 4, pp. 506–538, Jul. 2013.
[32] E. J. Norberg, R. S. Guzzon, J. S. Parker, L. A. Johansson, and L. A. Coldren, "Programmable photonic microwave filters monolithically integrated in InP–InGaAsP," *J. Lightw. Technol.*, vol. 29, no. 11, pp. 1611–1619, Jun. 2011.